PDL in Optical Links: a Model Analysis and a Demonstration of a PDL-Resilient Modulation

Arnaud Dumenil, Elie Awwad, *Member, IEEE*, Cyril Measson

***Abstract*—Optical communications networks include basic components such as EDFAs and WSSs that present a polarization gain imbalance. The gain imbalance at the component output depends on the incident state-of-polarization. This well-known phenomenon called Polarization Dependent Loss (PDL) is revisited in this paper and systematically analyzed within the framework of communications theory and practical achievable information rates. The rate impairment induced by PDL is discussed on an optical channel with distributed PDL and on a simplified equivalent lumped PDL channel. We have previously designed the New Spatially Balanced (NSB) signaling, an optimal 4D modulation based on this simplified model. We explore in this paper its performance through numerical simulations and experimentally over a transmission in a recirculating loop with in-line PDL. Experimental measurements confirm an accurate channel modeling and significant information rate gains brought by NSB that results in SNR gains of the order of 0.4dB at a practical transmission outage.**

***Index Terms*—Optical Fiber Communications, Multiplexing, MIMO systems, Polarization Dependent Loss**

NOTATIONS

Dimensions: $\mathbf{X} \in K^{n\times m}$ denotes a vector or matrix $\mathbf{X}$ of dimension $n \times m$, taking values in the field $K = \mathbb{R}$ or $\mathbb{C}$ and which conjugate transpose is denoted $\mathbf{X}^\dagger \in K^{m\times n}$.

Expectation, covariance and power: We denote $E[\mathbf{X}]$ the expectation of a random vector $\mathbf{X}$ over any field and any dimension. The covariance matrix of $\mathbf{X} \in \mathbb{C}^{n\times 1}$ for $n > 0$ integer is denoted $\mathbf{K_{XX}} = E\left[(\mathbf{X}\mathbf{X}^\dagger)\right]$ for zero-mean $\mathbf{X}$ and $P_X = \text{trace } \mathbf{K_{XX}}$ is the power of $\mathbf{X} \in \mathbb{C}^{n\times 1}$.

Particular distributions: A random vector $\mathbf{X} \in \mathbb{C}^{n\times 1}$ that follows a circularly-symmetric complex Gaussian noise with mean $\mathbf{A} \in \mathbb{C}^{n\times 1}$ and covariance matrix $\mathbf{B} \in \mathbb{C}^{n\times n}$ is denoted $\mathcal{CN}(\mathbf{A}, \mathbf{B})$. The uniform distribution over F is denoted $\mathcal{U}(F)$.

I. INTRODUCTION

In coherent optical fiber transmission networks, Polarization Dependent Loss (PDL) is a linear, non-unitary impairment expected to have a strong impact in next-generation systems [1]. For instance, novel Wavelength Selective Switches (WSSs) with sharp filtering can experience up to 0.6dB of PDL per port, a value that can also depend on the assigned attenuation on a given port. Typical operational links include 16 Reconfigurable Optical Add Drop Multiplexing (ROADM) nodes with 2 WSSs each, hence resulting in an average PDL exceeding 2dB [2]. In Fig. 1, we represent this simplified version of a link with n concatenated spans including a portion of l kilometers of fiber, followed by a PDL element and a PDL-free Erbium-Doped Fiber-Amplifier (EDFA) plotted as a triangle. The PDL elements here typically capture the WSSs effect, and the EDFAs add noise in a distributed manner along the link. Note that optical fibers do not add PDL, but the discrete elements along the link do. This first basic illustration serves as a starting point and is later mathematically modeled and then analyzed.

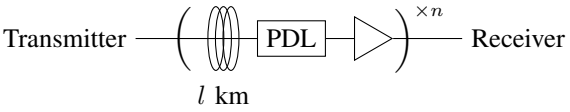

Fig. 1: Optical description of n concatenated spans including a long distance l of fiber, a PDL element and an EDFA represented with a triangle.

In this paper, we first develop the model of a single PDL element and concatenate them to form an optical link with distributed elements that we will call a PDL channel. We carefully analyze this channel and precisely determine the distribution of its characterizing parameters. Second, we elaborate on the performance of the PDL channel based on the mentioned models, either using a single, lumped, PDL transfer matrix or on the distributed link itself with an SNR penalty analysis. The achievable information rate of standard polarization-multiplexed (PolMux) QAM modulation is compared to the New Spatially Balanced (NSB) scheme recently introduced in [3] by the authors. Compared to other PDL compensating techniques, such as space-time codes [4], [5], [6], signalings requiring channel state information [7], [8] or modulation on different carriers [9], our optimal single-timeslot 4D signaling was designed to be robust to PDL while keeping the same degrees of freedom that are the in-phase and quadrature components of a PolMux signal on one carrier, and with no feedback on the channel. Additionally, for the first time the performance of the 2-timeslot 8D Silver code [4] over a channel with distributed PDL is later numerically evaluated. Eventually, we measure the performance of NSB compared to standard QAM in an experiment with a recirculating loop having inline PDL and demonstrate its interest for PDL resilience.

A. Dumenil is with Nokia Bell Labs France, route de Villejust, 91620 Nozay. E-mail: arnaud.dumenil@nokia-bell-labs.com

E. Awwad, C. Measson were with Nokia Bell Labs. E. Awwad is now with the Department of Communications and Electronics of TELECOM Paris, 16 place Marguerite Perey, 91120 Palaiseau.

Manuscript received Jan. 15, 2020; revised Apr. 28, 2020.

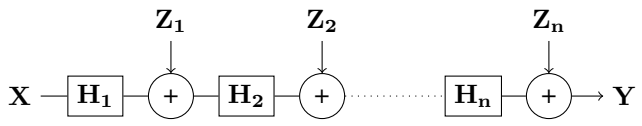

Fig. 2: Block representation of a concatenated chain of n PDL elements. Each span i is modeled as a matrix $\mathbf{H_i}$ (fiber, PDL element) and added noise $\mathbf{Z_i}$ (due to the amplifier).

II. Modeling of a Channel with PDL Elements

After presenting the PDL element modeling, we derive in this section the PDL channel model.

A. PDL modeling at the elementary component scale

Discrete components along an optical link may behave differently depending on the incident polarization. On a discrete component scale, if the gain associated with the first polarization is g_1 and the gain with the second one g_2, in general $g_1 \neq g_2$. Assuming that the two gains are along two orthogonal axes and an incident polarization-multiplexed signal $\mathbf{X}$ has its polarization tributaries aligned with its two axes, the output signal is $\mathbf{D_{el}X}$ [15, pp. 297-307] where $\mathbf{D_{el}} = \text{diag}\{g_1; g_2\}$ is a diagonal matrix with diagonal entries g_1 and g_2. As a short hand we say that the signal is aligned to the PDL element, in other words we identify the PDL element with its two gains axis. In general though, the signal meets the PDL element with a random state-of-polarization (SOP) with respect to a given frame of reference. Similarly, the output signal may be randomly orientated with respect to the reference. Hence, a basic PDL element can be modeled as

$$\mathbf{H_{el}} = \mathbf{U_{el}}\mathbf{D_{el}}\mathbf{V_{el}} \tag{1}$$

where $\mathbf{U_{el}}$ and $\mathbf{V_{el}}$ are two unitary matrices taken uniformly at random (depicting the uniform distribution of the input and output SOPs in the Poincaré sphere). Two different models may be employed to take into account the gain imbalance in $\mathbf{D_{el}} = \text{diag}\{g_1; g_2\}$.

1) Applying the loss over one polarization axis, typical convention for passive components, yielding $\mathbf{D}_\epsilon = \text{diag}\{1; \sqrt{\epsilon}\}$ with $\epsilon \in [0, 1]$ and leading to a loss of the total energy.
2) For active components, a total energy conservation can be assumed, yielding $\mathbf{D}_\gamma = \text{diag}\{\sqrt{1+\gamma}; \sqrt{1-\gamma}\}$ with $\gamma \in [0, 1]$.

In both cases, we refer to the difference of gains in dB.

Definition 1: The PDL value is defined as the decibel (dB) gain imbalance squared ratio of the diagonal elements of $\mathbf{D}$ and is denoted $\Lambda = 10\log_{10}(\max(g_1; g_2)^2/\min(g_1; g_2)^2)$. Note that when $\epsilon = 1$ or $\gamma = 0$, the PDL value is $\Lambda = 0$ dB. In this case, the component's two polarization gains are identical and there is no PDL. Eventually, the model 1 has a loss of energy $\text{trace}(\mathbf{H_{el}}\mathbf{H_{el}}^\dagger) = \text{trace}(\mathbf{D_{el}}^2) = 1+\epsilon$ compared to the model 2 that is energy conserving with $\text{trace}(\mathbf{H_{el}}\mathbf{H_{el}}^\dagger) = 2$.

B. Concatenation of discrete PDL elements

Along an optical link, a polarization-multiplexed signal is likely to encounter several cascaded PDL elements, typically EDFA amplifiers or WSSs, which impairments accumulate. Due to the random orientation of the components, the signal experiences a tempered effect that is different from the sum of all the PDL elements. In our model, we consider the channel as a concatenation of spans where each span is made of a fiber of a given length l km, a PDL element and an EDFA compensating fiber loss and adding amplified spontaneous emission noise. The model is represented in Fig. 1 where we delimit the span by brackets.

A block diagram of this physical model is depicted in Fig. 2. We consider n spans where each fiber and PDL element are embodied in the matrix $\mathbf{H_i}$ and the EDFA is replaced by an additive white Gaussian complex noise $\mathbf{Z_i} \sim \mathcal{CN}(\mathbf{0}, \mathbf{I})$ with unit variance per polarization. The fiber loss and insertion loss of the PDL element are assumed to be perfectly compensated for by the gain of the amplifier, $\mathbf{H_i} = \mathbf{U_i}\mathbf{D_i}\mathbf{V_i}$ are hence defined according to model 2. Moreover, we intentionally discard dispersive effects (chromatic dispersion (CD) and polarization mode dispersion (PMD)). CD can be perfectly compensated for in the electronic domain, whereas PMD is not modeled in this work as most novel transmission fibers exhibit very low PMD (around $0.01\text{ps}/\sqrt{\text{km}}$) which can be neglected even for long transmissions and high symbol rates. The study of the influence of moderate to high PMD values on the evolution of PDL, already initiated in [10], [11], [12] is left for a future work. Under these assumptions, and similarly to [13], [14] the transmitted vector $\mathbf{X}$ propagates from left to right in Fig. 2 and the resulting output vector $\mathbf{Y}$ is given by:

$$\begin{aligned}\mathbf{Y} &= \mathbf{Z_n} + \mathbf{H_n}(\mathbf{Z_{n-1}} + \mathbf{H_{n-1}}(\cdots(\mathbf{Z_2} + \mathbf{H_2}(\mathbf{Z_1} + \mathbf{H_1X}))\cdots) \\ &= \left[\prod_{i=n}^{1}\mathbf{H_i}\right]\mathbf{X} + \left[\sum_{i=1}^{n}\left(\Pi_{j=n+1}^{i+1}\mathbf{H_j}\right)\mathbf{Z_i}\right] \\ &= \mathbf{HX} + \mathbf{Z}\end{aligned} \tag{2}$$

with $\mathbf{H_{n+1}} = \mathbf{I}$, $\mathbf{H} = \Pi_{j=n}^{1}\mathbf{H_j}$ being the channel transfer matrix resulting from the product of all spans, and the resulting noise $\mathbf{Z}$ is still a zero-mean Gaussian complex noise but with covariance $\mathbf{K_{ZZ}} = \sum_{i=1}^{n}\mathbf{P_i}\mathbf{P_i}^\dagger$, where $\mathbf{P_i} = \Pi_{j=n+1}^{i+1}\mathbf{H_j}$. Hence, a link with distributed PDL elements, called a *PDL channel*, behaves as a single-element PDL channel with an equivalent Λ aggregating the ones of the elementary PDL-impaired components, along with a correlated noise $\mathbf{Z}$. As done for the elementary PDL matrix in Eq. 1, we substitute the channel matrix $\mathbf{H}$ by its Singular Value Decomposition (SVD) $\mathbf{Y} = \mathbf{UDVX} + \mathbf{Z}$. For simplicity, we left-multiply by $\mathbf{U}^{-1} = \mathbf{U}^\dagger$ unitary and incorporate it in the noise, that remains Gaussian but with covariance $\mathbf{U}^\dagger\mathbf{K_{ZZ}}\mathbf{U}$. We still denote this noise $\mathbf{Z}$ and redefine $\mathbf{Y} := \mathbf{U}^{-1}\mathbf{Y}$, such that we can write $\mathbf{Y} = \mathbf{DVX} + \mathbf{Z}$. Then there exists [15, pp. 71-72] $\phi, \delta, \alpha, \beta \in \mathbb{R}$ such that $\mathbf{Y} = e^{i\phi}\mathbf{D}\mathbf{B}_\delta\mathbf{R}_\alpha\mathbf{B}_\beta\mathbf{X} + \mathbf{Z}$. The $\mathbf{R}$ is a real rotation matrix and the $\mathbf{B}$ matrices are diagonal phase retardance matrices defined by

$$\mathbf{R}_\alpha = \begin{pmatrix}\cos\alpha & -\sin\alpha \\ \sin\alpha & \cos\alpha\end{pmatrix} \text{ and } \mathbf{B}_\beta = \begin{pmatrix}e^{i\beta} & 0 \\ 0 & e^{-i\beta}\end{pmatrix}. \tag{3}$$

Commuting the diagonal matrices $\mathbf{D}$ and $\mathbf{B}_\delta$, and left-multiplying by the the inverses of $\mathbf{B}_\delta$ and $e^{i\phi}$ (conserving

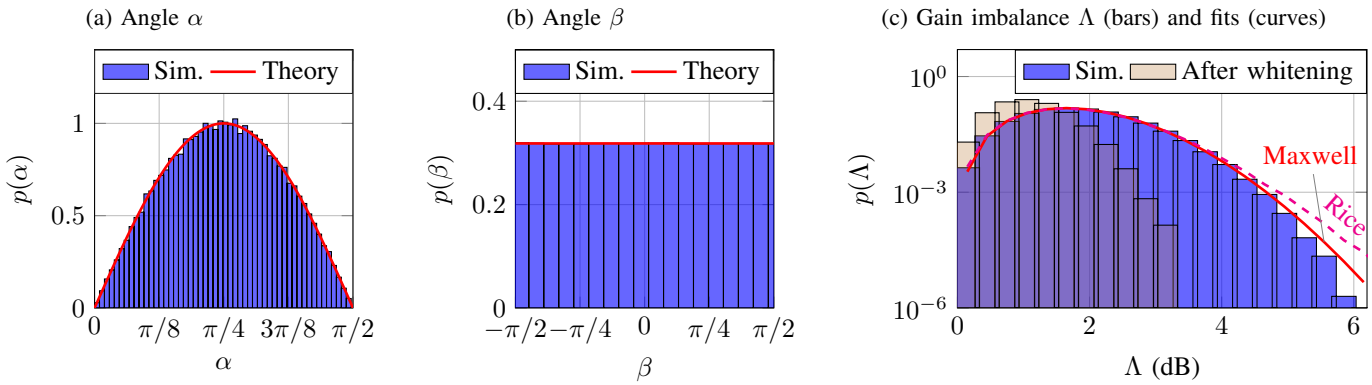

Fig. 3: Distribution of the equivalent channel parameters for 10^6 simulated PDL channel with $n = 25$ spans including randomly oriented PDL elements of $\Lambda_i = 0.4$dB each with the theoretical fits (red) and an alternative Λ fit (dashed magenta).

the noise properties), we redefine again for simplicity $\mathbf{Y} := \mathbf{B}_\delta^{-1}\mathbf{Y}$ and $\mathbf{Z} := \mathbf{B}_\delta^{-1}\mathbf{Z}$ to end up with the equivalent form:

$$\mathbf{Y} = \mathbf{D}\mathbf{R}_\alpha\mathbf{B}_\beta\mathbf{X} + \mathbf{Z} \tag{4}$$

The total gain values in the matrix $\mathbf{D} = \text{diag}\{g_1; g_2\}$ depend on the evolution of the polarizations between the individual PDL elements. It is worthy to note that the trace of $\mathbf{H}\mathbf{H}^\dagger$ is not constant for random drawings of concatenated fiber sections in the defined model that considers a constant-gain amplification scheme at EDFAs. We shall see in the performance analysis section that this hypothesis has an impact on the measured penalties, and we will compare it to a constant-output-power amplification scheme. We then rescale $\mathbf{D}$ to match again the PDL model 2 with parameter γ. Finally, apart from the colored noise, the global channel transfer matrix $\mathbf{H}$ can be redefined with three parameters: the gain imbalance Λ (or equivalently γ) in $\mathbf{D}_\gamma$, and two angle parameters α and β in $(-\pi, \pi]$

$$\mathbf{H} := \mathbf{D}_\gamma\mathbf{R}_\alpha\mathbf{B}_\beta \tag{5}$$

The next section looks into the statistics of these parameters.

C. Channel statistics and impact of colored noise

The unitary matrices $\mathbf{U}$ and $\mathbf{V}$ are random. Indeed, since no direction is favored in the channel, the two unitary matrices are uniformly distributed in $\mathrm{U}(2)$ (the set of unitary matrices of order 2) with respect to the Haar measure [16]. The derivation of the Haar measure volume element [17] imposes β following $\mathcal{U}([0, 2\pi])$, the uniform distribution on the range $[0, 2\pi]$ and the probability density function of the angle $\alpha \in [0, \pi/2]$ is

$$p(\alpha) = \sin(2\alpha) \tag{6}$$

In Fig. 3a and Fig. 3b, the distribution of respectively the angle α and β restricted in $[-\pi/2, \pi/2]$ are extracted from 10^6 simulated PDL channels with $n = 25$ spans and shows the expected probability laws.

For a sufficiently large number of concatenated elements with identical PDL values, it is shown in [18] that the singular values squared ratio in decibel Λ of the equivalent channel $\mathbf{H}$ follows a Maxwellian distribution. The resulting distribution of $n = 25$ spans of randomly oriented PDL elements of $\Lambda_i = 0.4$dB each is represented in Fig. 3c. It shows a good fit between the actual singular values ratio distribution (blue) and the theoretical distribution [18] (red curve) computed from the empirical mean of the obtained PDL values. We used sufficiently large number n of elements so that the Maxwellian approximation is correct. The polarization scrambling by different fiber spans between the PDL elements slows down the evolution of the accumulated PDL. The global PDL of the channel is roughly equal to $0.92\Lambda_i\sqrt{n}$. Practical links are typically designed to be robust to worst case scenarios. The rule-of-thumb is to consider 3 times the average PDL value as the worst PDL the link can experience. For an example link constituted of 16 nodes with WSSs of 0.5dB of PDL each, the order of magnitude of the average link PDL is $0.5\sqrt{16} = 2$dB. Therefore, in the following section we take 6dB as an example value to illustrate the modulation format performance.

Now, we look into the impact of the correlated noise $\mathbf{Z}$. An equivalent channel model can be derived from Eq. 4 where we whiten the noise with $\mathbf{K}_{\mathbf{ZZ}}^{-1}$ the inverse of the covariance matrix of $\mathbf{Z}$. The distribution of the gain imbalance after noise whitening is represented in brown on Fig. 3c. The gain imbalance still follows a Maxwellian distribution but with a lower mean value. Indeed, while propagating along with the signal, the noise is also impacted by the PDL elements.

In reality, an uncertainty can impact the PDL introduced by optical components in a given link. Hence, we assume that our elementary PDL is given by a (not truncated) Gaussian distribution with mean 0.4dB and a variance σ_{el}^2 between 0 (fixed PDL element case) and 10^{-1} to check the validity of our model. We reported in table I the average of the link PDL Λ for 25-span channels in which elementary PDL are distributed as previously mentioned. We observe that for tight dispersion around the value of the fixed PDL element case, the average link PDL remains similar. But it becomes larger when PDL elements have a value that varies more. This has to be taken into account when designing a system subject to PDL effects.

D. Alternative and simplified emulation of a PDL channel

We present an alternative method to model the gain imbalance distribution inspired from wireless communications channel models that has a reduced emulation complexity. First,

(a) Rate vs. ρ for a Gaussian, DP-QPSK, and DP-16QAM input

(b) DP-QPSK rate at $\rho = 8$dB

(c) NSB- and Silver-QPSK rate at $\rho = 8$dB

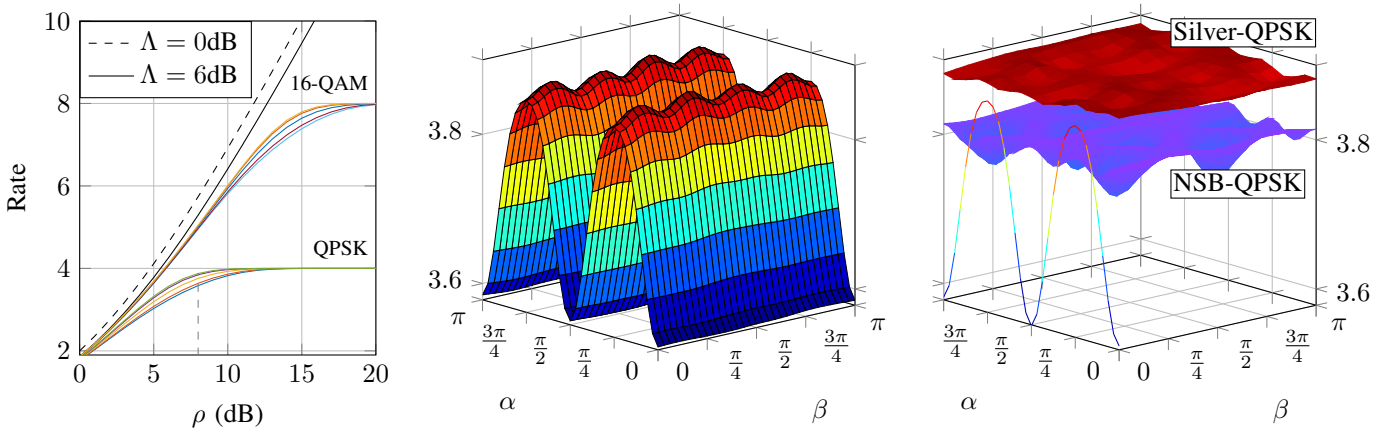

Fig. 4: Information rates in bits/symbol on the lumped PDL channel with $\Lambda = 6$dB for various angles α and β.

σ^2_{el}	0	10^{-2}	10^{-1}
$E[\Lambda]$	1.852	1.853	1.907

TABLE I: Average PDL value $E[\Lambda]$ of the equivalent channel for different elementary PDL dispersions varying around a mean value of 0.4dB.

note that the classical Rayleigh channel modeled by a transfer matrix with coefficients each following a $\mathcal{CN}(0,1)$ distribution differs from the optical channel. Indeed, one polarization totally dropping in a polarization-multiplexed propagation in a fiber is unrealistic but total fading is possible in a multi-antenna Rayleigh channel transmission. Therefore, we add the equivalent of a line-of-sight component to it, illustrating the direct path of the source in a guided medium.

$$\mathbf{H} = a\mathbf{G} + b\mathbf{I_2} \tag{7}$$

where $\mathbf{G}$ is the Rayleigh fading channel transfer matrix, a and b are in $[0,1]$. For $b = 0$ this is the Rayleigh fading channel again. For $a = 0$ the channel is deterministic. We omit these two extreme cases. The modeled channel is then equivalent to a Rice fading channel.

For $b \gg a \neq 0$, the dB squared ratio of the singular values Λ of $\mathbf{H}$ has a *Maxwellian-like* shape plotted in Fig. 3c (magenta dashed line). The figure shows a good accordance down to $p(\Lambda) = 10^{-3}$ between the proposed modeling and the Maxwellian fit curve with identical average value. Note that in section II-C, the Maxwell distribution appeared for *concatenated* PDL elements in sufficiently large number $n > 15$. Here, the distribution displayed in magenta dashed line is the one of a *single* element with transfer matrix $\mathbf{H}$ from Eq. 7. Instead of precisely taking into account the model of each PDL element and concatenating them, the resulting channel may be replaced by a transfer matrix following the Rice distribution and shows a good approximation of the real resulting PDL values. This modeling offers a reduced simulation complexity and gives almost the same statistics of a PDL channel. The average value of the dB singular value squared ratio Λ of a Rice channel is given by

$$E[\Lambda] \approx 6\ln(10) \times a/b \tag{8}$$

This is the formula used to fit the simulated PDL distribution in Fig. 3c from the mean of the drawn values. Exact derivation of the singular value distribution is possible using the complex expression of the joint distribution in [19]. Finally, the unitary matrices appearing in the SVD are uniformly distributed in the unitary group.

III. Impact of PDL on Channel Capacity and Design of Resilient 4D Modulations

In this section, we analyze a new modulation format that is resilient to PDL. For simplicity, we consider a fixed gain imbalance value, all possible polarization states and an uncorrelated noise. In this scenario, the scheme is designed to increase the rate associated with the worst orientation. In section IV, we complete the rate analysis by reintroducing the distributed channel with correlated noise to compare different modulation schemes.

A. PDL impairment and discrete modulations angle sensitivity

As discussed in [20], the well-known lumped PDL channel capacity is impacted by the PDL value. Fig. 4a firstly shows the capacity of a PDL channel (black curves) as a function of the Signal-to-Noise Ratio (SNR) ρ reproduced from [20] using a Gaussian input for entropy maximization. This represents the ultimate limit of communication of this 2×2-MIMO channel. Observe that the capacity with 6dB of PDL (full line) is reduced compared to a PDL-free channel (dashed line). The focus on 6dB of PDL is commonly used as it is the value corresponding to a 10^{-5} outage probability in a link with average PDL of 2dB. The information rates of DP-QPSK (lower curves) and DP-16QAM (top curves converging to 8 bits/symbol) schemes are represented in the same figure as a function of the SNR and for various SOPs. Note the additional rate variation that strongly depends on the incident

SOP. Typically [20], the lower curve for each format is met for $\alpha = 0$ modulo $\pi/2$ and the best rate is reached for $\alpha = \pi/4$. There is in particular a great dependence in the incident angle α and a lower dependence in the second angle β. This is depicted in details in Fig. 4b with the information rate of DP-QPSK represented as a function of the two angle parameters, and still for $\Lambda = 6$dB. A similar profile is found for any modulation M-QAM with arbitrary order of modulation M.

The average information rate of a PDL channel is the mean of the presented values in Fig. 4b weighted by the probability laws of the parameters discussed in section II-C. A lot of efforts is currently made in order to reduce the aforementioned angles dependency. In particular there is a need to increase the worst capacity here obtained for α angles multiple of $\pi/2$. Indeed, optical systems are designed to be robust to a worst case scenario. In other words, the transmission has to be guaranteed even in the parameters' worst configuration.

B. Design of modulations for PDL-resilience

In order to mitigate this angle dependency in a PDL channel, the Silver code has first been proposed [4] and studied [21]. This is a 2-timeslot modulation that is the best performing modulation known for PDL mitigation. An alternative two-timeslot code with a simpler structure and similar performance has also been proposed [6]. These 8D modulations though imply a higher decoding and equalization complexity making it unpractical in real transmission systems. The authors then presented in [3] a low-complexity 4D modulation robust by design to PDL called the *New Spatially Balanced* (NSB) signaling. This signaling has been found based on a numerical optimization of the worst information rate. It represents the best way to encode QAM symbols with a unitary matrix encoding, with no additional degrees of freedom and without knowledge of the channel at the transmitter. The used degrees of freedom are the same as the regular DP-QAM one, namely the in-phase and quadrature dimensions on the two orthogonal polarizations of the optical field.

The NSB signaling information rate is presented in Fig. 4c as a function of the two angle parameters, using QPSK as base modulation to encode. The profile of the DP-QPSK is plotted as a reference amplitude scale. Observe the increase of the rate for a significant number of angle pairs. In particular, the rates for α multiples of $\pi/2$ are significantly increased, by around 70% of the DP-QPSK amplitude range. Again, by construction the minimum rate over the grid is the maximum worst rate of all possible unitary 4D transforms. Additionally, we display in the same figure the rate of the Silver encoded QPSK corresponding to the higher plateau. It represents the upper limit of achievable information rate in a PDL channel to be able to appreciate the NSB signaling performance.

The NSB encoding matrix has been found manipulating the lumped PDL model, and in the following sections we propose to investigate its performance on a multi-span channel. We first present a problematic related to EDFAs in a distributed link to later comment on the NSB signaling results.

IV. Performance Analysis on Distributed PDL

A. Impact on the SNR of the amplifiers modes

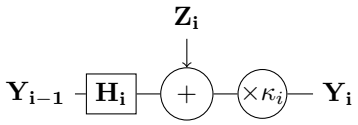

Fig. 5: Span representation with EDFAs in COP mode. The rescaling factor κ_i ensures identical power at each span output.

In optical links EDFAs are used inline in order to boost the signal that has lost power along its propagation in spans of up to 100 kilometers. To model it, we consider two modes, either they work with a fixed *gain*, or with a fixed *Constant Output Power* (COP). In this section we study the difference of behavior between the two.

When designing a system, the number of spans the signal will go through is taken into account. Namely, in a submarine cable for instance, the link between the transmitter and the receiver is constituted of a number of spans n, it means the signal will propagate on a long fiber distance and then re-amplified n times. Assuming each amplifier produces noise according to a Gaussian process $\mathcal{CN}(\mathbf{0}, \mathbf{I})$, in order to target a given SNR ρ^* at the receiver, the power at the transmitter should be of

$$P_X = 2n\rho^* \tag{9}$$

The targeted SNR cannot be guaranteed as the PDL elements may either amplify or attenuate the signal depending on the PDL elements random orientation at the input of the element. Indeed, the power modifying matrix $\mathbf{H_i}$ makes the total output power a random variable and impossible to exactly predict when designing a system. Then, in what follows we distinguish when applicable between the notations of the target SNR ρ^* and the effective SNR ρ.

Amplifiers in COP mode on the other hand make sure that the power at the output of the amplification at each span is set to a fixed value P_0. In practice, $P_0 = P_X$, the power of the signal at the transmitter. In Fig. 5 the modeling of an amplifier with constant output power is represented. Again, we omitted here the (static) amplification gain the amplifier is designed for: we assume it amplifies the input signal $\mathbf{Y_{i-1}}$ to compensate for the total power loss it has been subject to in span $i-1$. The transfer matrix $\mathbf{H_i}$ captures the effects of the current span i including its orientation but excluding the total power loss and compensation just described. The scaling factor κ_i is meant to rescale the output power of the amplifier to a set value. This scaling factor is expressed as

$$\kappa_i = \sqrt{\frac{P_0}{P_{H_i Y_{i-1}} + 2}} \tag{10}$$

the term 2 coming from the noise power added by the amplifier and $P_{H_i Y_{i-1}}$ the power of the signal $\mathbf{Y_{i-1}}$ coming from the previous span and modified by the current span matrix $\mathbf{H_i}$.

Assume now that we have a link with n spans that does not contain any PDL. Then the scaling factor is a constant $\kappa = \sqrt{P_0/(P_0+2)}$ in the case of a PolMux transmission. At

(a) SNR degradation with EDFAs in COP mode with QPSK (red) and 16QAM (blue) operating regions

(b) Rate occurrences for 5000 randomly distributed channels with 15 spans of elementary PDL 1.1dB at SNR 9.2dB.

(c) Outage verification for n spans for PDL elements of 0.6dB (PDL model 2 and COP mode)

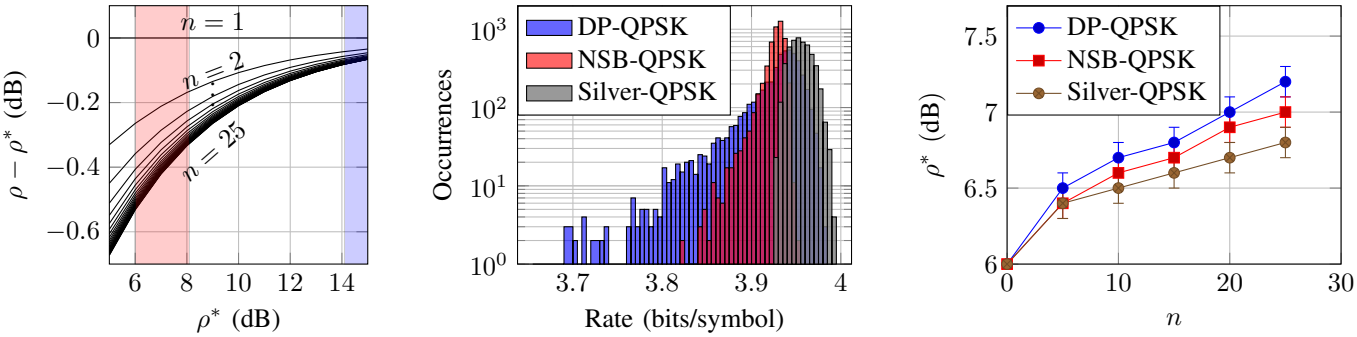

Fig. 6: Distributed channel impact on the information rate for various modulation schemes and on the effective SNR ρ.

the end of the link the power of the signal $\mathbf{HX}$ propagated through the equivalent channel $\mathbf{H}$ and the total noise $\mathbf{Z}$ are

$$P_{HX} = (\kappa^2)^n P_0 \text{ and } P_Z = 2\sum_{i=1}^{n}(\kappa^2)^i \tag{11}$$

In Fig. 6a the SNR degradation $\rho^* - \rho$ (also known as the droop effect [22]) is depicted for various numbers n of spans with no PDL as a function of the targeted SNR ρ^* in the sense of formula 9. The value of ρ is the effective SNR defined as the ratio between the two terms of expression 11. We superimpose the areas of operation of the QPSK and 16-QAM represented with an example targeted pre-bit decoding BER of 10^{-2}. Observe that the QPSK scheme is more impacted by the COP mode of the amplifier and requires additional power at the transmitter to take into account the SNR degradation shown in the figure. Even with no PDL, the constant output power of the EDFA degrades the effective SNR at the receiver.

B. Rate analysis on the distributed PDL channel

We now propose to compare the performance of the channel in terms of verified outage condition. From an optical system operator's perspective, because a distributed channel is random, it may be impossible to guarantee information transmission in 100% of the time. This is depicted in Fig. 6b with the rate distribution of 5000 distributed PDL channels with $n = 15$ randomly oriented PDL elements modeled with $\mathbf{D}_\gamma$ with $\Lambda = 1.1$dB of PDL and EDFAs in constant gain mode using DP-, NSB-, and Silver-encoded QPSK at the same SNR $\rho^* = 9.2$dB. As can be expected, the rates are not a single value as in the previous lumped PDL case but rather distributed. A rate realization depends on the equivalent resulting channel gain imbalance as well as the signal incident orientation to it. Rates depend also on the total noise construction in the channel propagation. The distribution of the rates with the PDL model 1 or with EDFAs in COP mode are similar but with a shifted mean value. Observe that the NSB-QPSK (red) is as desired less impacted by the PDL channel with the minimum rate realization 0.13 bits/symbol larger than the one of the DP-QPSK (blue). The Silver-QPSK (gray) minimum rate is even larger, and its rate distribution is significantly more compact.

Based on this unpredictable characteristic of the information rate over a distributed PDL channel, it is useful to define a system outage probability condition and seek criteria that enable to verify them. In this work, we present the following outage condition based on information rates.

Definition 2: We say that a system meets the outage condition if the rates I below a given threshold value I_{th} happens with a probability of at most μ

$$P(I < I_{\text{th}}) \leq \mu \tag{12}$$

We compute the rate over 10^5 PDL channels with elementary PDL 0.6dB at n loops between 0 and 25 by increment of 5. We hence explore RMS PDL values up to 3dB. We test three different modulations: the regular DP-QPSK, the proposed NSB-QPSK, and the Silver-QPSK on 2 timeslots. We seek the SNR that first verifies the outage condition 12 with $\mu = 10^{-3}$ and $I_{\text{th}} = 3.6$ bits/symbol for the three modulations. This particular rate threshold value corresponds to the commonly-used coding rate of 0.9 in optical communications. Eventually, we use the PDL model 2, EDFAs are in COP mode and an ideal, maximum-likelihood, equalization and demapping is assumed at the receiver when computing the mutual information.

Fig. 6c displays the required target SNR at the receiver in order to respect the outage condition as the RMS PDL increases. For a given n, this is equivalent to increasing the launch power at the transmitter. The COP mode here guarantees the output signal $\mathbf{Y}$ to be at a set power value. With no PDL, the channel is just a SOP rotation and the three modulations check the outage condition for the same SNR. This can be seen in Fig. 6c as the three modulation curves originate from the same point at $n = 0$. When PDL is added, the outage condition validation is met for a higher SNR and differs depending on the modulation. Besides the addition of 5 PDL elements of 0.6dB, the steep increase from $n = 0$ to 5 may be understood from a sudden drop in the effective SNR according to Fig. 6a as DP-QPSK operating regions are strongly impacted by the EDFAs COP mode. This loss of SNR is translated in a global decrease of the information rates hence the requirement for even additional power at the

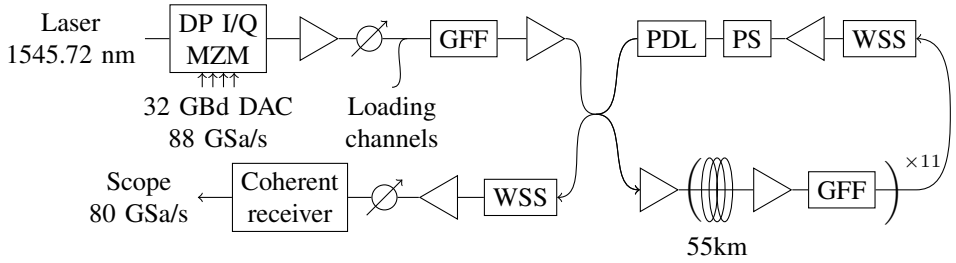

Fig. 7: Distributed PDL experimental setup: recirculating loop with in-line PDL preceded by a Polarization Scrambler (PS), 11x55km fiber spools and EDFAs. Gain Flattening Filters (GFF) and WSSs are inserted to ensure a flat C-band spectrum.

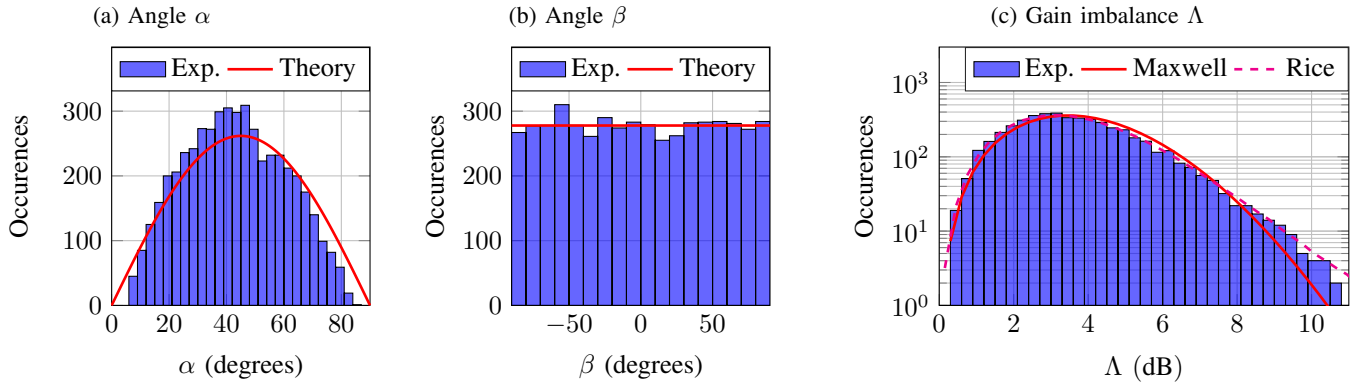

Fig. 8: Parameters distribution of 5000 channels constituted of $n = 15$ concatenated, randomly oriented, PDL elements of 1.1dB following the experimental setup in Fig. 7.

transmitter. Observe that the Silver-QPSK as expected is the best modulation of the three tested and gives the highest SNR relaxation of 0.4dB compared to DP-QPSK for 3dB of RMS PDL ($n = 25$). At this same PDL value, the NSB-QPSK enables a relaxation of 0.2dB of required SNR but for the same decoding complexity as the DP-QPSK. The gap between the DP-QPSK and the other two modulations tends to increase as the number of loop increases which shows their interest to be used in practice for PDL-resilience in optical links.

V. Experimental Validation of the Analytical Models and the NSB Signaling Resilience to PDL

We propose here to experimentally demonstrate the performance of the NSB signaling on a distributed PDL channel.

A. Adapted data-aided equalization scheme

By construction, the NSB signaling is a modulation for which the information on one polarization is dependent on the other. As for any 4d (or 8d) encoded modulation, the information is spread over all of the 4 (or 8) components of the signal. Therefore, the classical 2×2 constant modulus algorithm equalizer is not suitable because it assumes independent polarization streams. Consequently, we choose a pilot-based DSP approach [23] for channel estimation and equalization and compare the performance of standard DP and NSB-coded signals using the same DSP.

The processing chain consists in normalization and resampling of the two acquired complex signals, compensation of chromatic dispersion when needed, time and frequency synchronization, data-aided channel estimation and multi-tap MMSE equalization [24], followed by carrier phase noise compensation. The channel pilots are localized using a synchronization sequence at the forefront of the frame. For channel estimation, Constant Amplitude Zero Autocorrelation [25] (CAZAC) sequences of length l_c repeated n_{rep} times are used. For carrier phase noise estimation, a short sequence of random symbols are periodically inserted all along the frame. Finally, an information rate per polarization is computed as the mutual information between the equalized signal and the corresponding transmitted tributary. From the estimated channel, the global PDL Λ and the incident SOP are extracted through a singular value decomposition of the estimated channel matrix $\mathbf{H}$ at the central tap. The sent signals consist then of two complex vectors of 2^{14} symbols each including a real-valued 64-symbol synchronization sequence, $l_c = 64$-symbol CAZAC sequences repeated $n_{\text{rep}} = 10$ times, and the payload symbols where the first half is standard DP-QPSK modulated and the second half is NSB-QPSK coded. This frame structure enables a performance comparison between the two schemes for the same observed channel at each acquisition. For carrier phase recovery, we insert 8 QPSK pilots every 400 data symbols. The added pilots represent 6.25% of the total frame.

B. Channel statistics

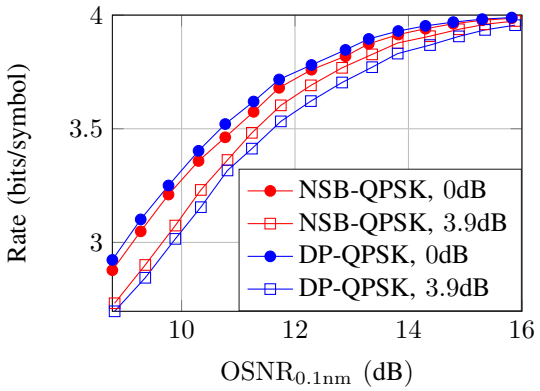

Fig. 9: Back-to-back rates in the presence of $\Lambda = 0$dB or 3.9dB of PDL in an aligned ($\alpha = 0$) configuration. The rate is plotted as a function of the OSNR measured in a bandwidth of 0.1nm at 32Gbaud.

The channel under test at 1545.72nm is modulated with polarization-multiplexed root-raised-cosine filtered 32GBaud signals with a roll-off of 0.01. The experimental setup is represented in Fig. 7 where the tested channel is inserted in a recirculating loop along with 87 loading channels covering the C-band. The loop consists of 11 spans of 55km Corning Vascade EX3000 fibers with $0.02\text{ps}\sqrt{\text{km}}$. Having a single PDL emulator, we set its PDL value at $\Lambda = 1.1$dB and inserted it in the loop preceded by a controllable polarization scrambler. With such low PMD value, the accumulated PDL will be flat over the bandwidth of the transmitted signal. The scrambler randomly changes the SOP for each loop. After 15 loops yielding a total distance of 9075km, the signal is acquired through a coherent receiver and a 80GSa/s scope.

A total of 5000 acquisitions are recorded to cover different channel states. In Fig. 8c, we show the statistics of the estimated overall gain imbalance Λ that fit well with the theoretical Maxwell distribution of mean $0.92 \times 1.1 \times \sqrt{15} = 3.9$dB [18]. Interestingly, the gain imbalance obtained from an emulated Rice channel with identical mean (magenta dashed curve) has a distribution that here matches more closely those experimental values. Fig. 8a shows the statistics of the rotation angle α defined in section II-C. The obtained circular-shaped distribution depicts a uniform sampling of the Poincaré sphere. The use of CAZAC sequences, optimal for uncorrelated noise channels, may explain the small deviation between the theoretical and experimental values of Λ and α since the noise is correlated. With no channel state knowledge at the transmitter, CAZAC sequences have been used for simplicity. Additionally, the extracted retardance angle β in $[-\pi/2, \pi/2]$ represented in Fig 8b is uniformally distributed as expected.

C. Performance of the New Spatially Balanced signaling

After measuring the observed channel statistics, as in [26] we focus on the information rates and compare them between the two modulation schemes. First, we evaluated the total rate over both polarization tributaries in a back-to-back experiment without PDL (circle markers). We see in Fig. 9 that the NSB-coded part suffers from a small penalty compared to standard DP-QPSK mainly due to imperfect phase estimation. Indeed, given that the NSB consists in mixing the in-phase and quadrature dimensions of the two polarizations, it has an increased sensitivity to phase recovery imperfections. At an OSNR of 13dB in 0.1nm corresponding to the measured value after 15 loops, the penalty is 0.0125bit/symbol.

While remaining in back-to-back, we add a 3.9dB loss (corresponding to the average overall PDL after 15 loops) over one polarization at the transmitter to emulate the aligned PDL case where the coding gains are expected to be the highest [3] and measure the total rate shown in squared markers. The rate enhancement is clearly illustrated over all the measured OSNR range. Next, we analyze the information rates per polarization after transmission over 9075km for all encountered Λ values and SOP states. For the NSB-coded part, the measured penalty in back-to-back at an OSNR of 13dB was added to assess the PDL-mitigation gain independently of imperfect phase recovery. Fig. 10a displays the statistics of all the measured rates per polarization for the two schemes. We notice a net worst case enhancement and a reduction of rate fluctuations for the NSB part. Finally, in Fig. 10b, we represent the measured rates of the most-impaired polarization for the NSB-QPSK and standard DP-QPSK as a function of the corresponding estimated PDL. The worst polarization rate is statistically higher for the NSB coded scheme (gray triangles) than for the standard DP one (black points). Again, the alleviation of the worst case is well observed when the joint 4D signaling is employed.

VI. Conclusion

In this paper, we build upon earlier works [3] on PDL modeling and PDL-resilient signalings that rely on the classical lumped model. In this work indeed, we take a step towards the implementation of our techniques. We systematically model the PDL channel as a distributed link with discrete components to better reflect the practice of optical networks. We first analyzed the limits of communications on the lumped PDL channel showing the gain imbalance impact with 0.6bit/s/Hz in capacity loss with a PDL of 6dB. Additional rate losses have to be expected with practical DP-M-QAM modulations, motivating the construction of the PDL-resilient NSB signaling that offers a 70% minimum rate increase. Nevertheless, we showed that a real-life PDL channel cannot be summarized as the lumped PDL channel only. We indeed presented the distributed PDL impact as well as the orthogonal issue of the SNR degradation appearing in distributed links due to EDFAs in COP mode. This SNR degradation reaches up to 0.6dB in the considered operating regions. We then proposed a comparison between the NSB signaling, the standard DP-QPSK scheme and the PDL-robust Silver code on a distributed link with an outage study. The NSB signaling and the Silver code offered a reduction of 0.2dB and 0.4dB, respectively, of required SNR for the considered outage condition compared to standard QPSK. Finally, we experimentally tested the NSB for

(a) Rate per polarization distribution

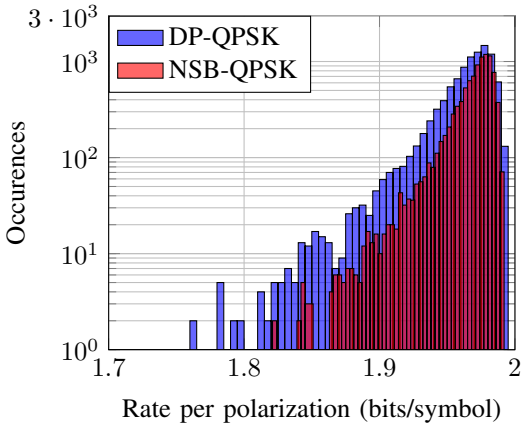

(b) Worst polarization rate function of the PDL

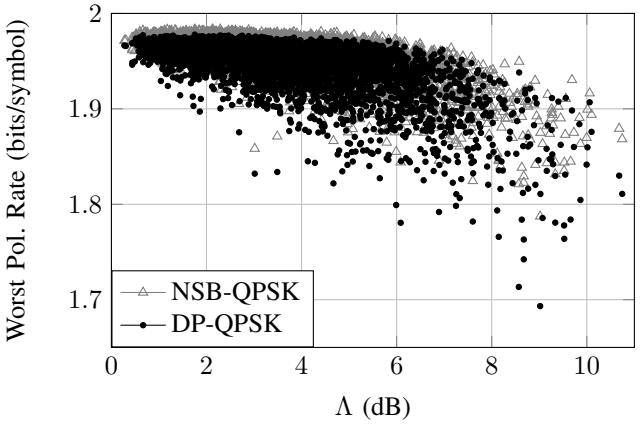

Fig. 10: Polarization rate statistics of 5000 channels with $n = 15$ randomly oriented PDL elements of 1.1dB of PDL.

PDL mitigation in an optical link with distributed PDL. Even though it is more sensitive to phase recovery imperfection, the worst polarization rates appeared to be higher than the DP-QPSK scheme ones. This a first demonstration of PDL resilience in the context of a real optical link composed of discrete components.

REFERENCES

[1] H.-M. Chin, D. Charlton, A. Borowiec, M. Reimer, C. Laperle, M. O'Sullivan, and S. J. Savory "Probabilistic Design of Optical Transmission Systems," *J. Lightwave Technol.*, vol. 35, no. 4, pp. 931-940, 2017.

[2] L. E. Nelson, C. Antonelli, A. Mecozzi, M. Birk, P. Magill, A. Schex, and L. Rapp, "Statistics of polarization dependent loss in an installed long-haul WDM system," *Opt. Express*, vol. 19, no.7, pp. 6790-6796, 2011.

[3] A. Dumenil, E. Awwad, and C. Measson, "Rate Optimization Using SO(4) Transforms for PDL Mitigation," *2018 European Conference on Optical Communication (ECOC)*, Dublin, paper W2D.4, 2019.

[4] S. Mumtaz, G. Rekaya-Ben, and Y. Jaouën, "Space-time codes for optical fiber communication with polarization multiplexing," *2010 IEEE International Conference on Communications (ICC)*, 2010.

[5] A. Andrusier, E. Meron, M. Feder, and Mark Shtaif, "Optical implementation of a space–time-trellis code for enhancing the tolerance of systems to polarization-dependent loss," *Opt. Lett.*, vol. 38, no.2, pp. 118-120, 2013.

[6] T. Oyama, G. Huang, H. Nakashima, Y. Nomura, T. Takahara, and T. Hoshida, "Low-Complexity, Low-PAPR Polarization-Time Code for PDL Mitigation," *2019 Optical Fiber Communication Conference (OFC)*, paper W3H.1, 2019.

[7] J. C. Cartledge et al., "Compensation of Polarization Dependent Loss by Optimizing the Transmitted State-of-Polarization for 140 Gbit/s DP-QPSK," *2016 Advanced Photonics Congress (SPPCom)*, paper SpM3E.4, 2016.

[8] G. Huang et al., "Efficient Polarization Dependent Loss Monitoring and Compensation in Coherent Transmission System," *2018 European Conference on Optical Communication (ECOC)*, Rome, paper We2.40, 2018.

[9] T. Tanimura, T. Oyama, H. Nakashima, and J. C. Rasmussen, "PDL-Tolerant Signal Generation by Digital Spectrum Slicing and Polarization Control," *2015 Optical Fiber Communication Conference*, paper Th2A.14, 2015.

[10] N. Gisin, B. Huttner, "Combined effects of polarization mode dispersion and polarization dependent losses in optical fibers," *Optics Communications*, vol. 142, no. 1–3, pp. 119-125, 1997.

[11] Xiang Liu and Fred Buchali, "Intra-symbol frequency-domain averaging based channel estimation for coherent optical OFDM," *Opt. Express*, vol. 16, no. 26, pp. 21944-21957, 2008.

[12] T. Hirooka et al., "PMD-induced crosstalk in ultrahigh-speed polarization-multiplexed optical transmission in the presence of PDL," *J. Lightwave Technol.*, vol. 29, no. 19, pp. 2963-2970, 2011.

[13] A. Elamari et al. "Polarisation Dependent Loss of concatenated passive optical components," *1996 Symp. Optic. Fiber Measurements (SOFM)*, pp. 163-166, 1996.

[14] Z. Tao et al., "A fast method to simulate the PDL impact on dual-polarization coherent systems," *IEEE Photon. Technol. Lett.*, vol. 21, no. 24, pp. 1882-1884, 2009.

[15] J. N. Damask, *Polarization Optics in Telecommunications*. New York, NY, USA: Springer-Verlag, 2005.

[16] A. Edelman, "Eigenvalues and Condition Numbers of Random Matrices," Ph.D. dissertation, Dept. Mathematics, MIT, Cambridge, MA, USA, 1989.

[17] M. Ozols, "How to generate a random unitary matrix," lecture notes from March 16, 2009, accessible online.

[18] A. Mecozzi, M. Shtaif, "The statistics of polarization-dependent loss in optical communication systems," *IEEE Photon. Technol. Lett.*, vol. 14, no. 3, pp. 313-315, 2002.

[19] A. Maaref and S. Aissa, "Joint and Marginal Eigenvalue Distributions of (Non)Central Complex Wishart Matrices and PDF-Based Approach for Characterizing the Capacity Statistics of MIMO Ricean and Rayleigh Fading Channels," *IEEE Trans. on Wireless Comm.*, vol. 6, no. 10, pp. 3607-3619, 2007.

[20] A. Dumenil, E. Awwad, and C. Méasson, "Polarization Dependent Loss: Fundamental Limits and How to Approach Them," *Advanced Photonics 2017 (SPPCom)*, paper SpM4F.1, 2017.

[21] E. Awwad, "Emerging Space-Time Coding Techniques for Optical Fiber Transmission Systems", Ph.D. Dissertation, Telecom ParisTech, Paris, France, 2015.

[22] J. Antona, A. C. Meseguer, and V. Letellier, "Transmission Systems with Constant Output Power Amplifiers at Low SNR Values: A Generalized Droop Model," *2019 Optical Fiber Communications Conference and Exhibition (OFC)*, San Diego, CA, USA, paper M1J.6, 2019.

[23] M. Mazur, J. Schröder, A. Lorences-Riesgo, T. Yoshida, M. Karlsson, and P. A. Andrekson, "Overhead-optimization of pilot-based digital signal processing for flexible high spectral efficiency transmission," *Opt. Express*, vol. 27, no. 17, pp. 24654-24669, 2019.

[24] M. Kuschnerov, M. Chouayakh, K. Piyawanno, B. Spinnler, E. de Man, P. Kainzmaier, M. S. Alfiad, A. Napoli, and B. Lankl, "Data-Aided Versus Blind Single-Carrier Coherent Receivers," *IEEE Photon. Journal*, vol. 2, no. 3, pp. 387-403, 2010.

[25] D. Chu, "Polyphase codes with good periodic correlation properties (Corresp.)," *IEEE Trans. on Information Theory*, vol. 18, no. 4, pp. 531-532, 1972.

[26] A. I. A. El-Rahman and J. C. Cartledge, "Implications of Distributed Link Polarization-Dependent Loss on Bitwise Achievable Information Rates for Probabilistically Shaped and Uniform DP 64-QAM," *J. Lightwave Technol.*, vol. 37, no. 4, pp. 1187-1194, 2019.